

## SILICONE RESINS FILLED WITH ALUMINA NANOPARTICLES FOR IMPREGNATION OF ELECTRICAL MOTORS TITLE

A.M. Scamardella <sup>1,2</sup>, C. Petrarca <sup>3</sup>, A. Masucci <sup>4</sup>, E. Amendola <sup>1,2\*</sup>

<sup>1</sup> Institute of Composite and Biomedical Materials, CNR-Italy's National Council of Research, P.le E. Fermi 1, 80055 Portici (Na), Italy

<sup>2</sup> Technological District on Engineering of polymeric and composite Materials and Structures, IMAST S.C.A.r.L., P.le E. Fermi 1, 80055 Portici, Naples, Italy

<sup>3</sup> Department of Electrical Engineering, University of Naples "Federico II, Via Claudio 21, 80125 Naples, Italy

<sup>4</sup> Ansaldo Breda, Via Argine 425, 80147 Naples, Italy

\* amendola@unina.it

**Keywords:** silicone resin, ceramic nanofiller, nanodielectrics

### Abstract

*In the present paper, a new impregnation system for rotor and stator windings of medium and high power traction motors are obtained using silicone thermosetting resins and alumina nanoparticles. Silicone nanocomposites are prepared by combined dispersion techniques, namely mechanical mixing and sonication. Results about thermal, mechanical and electrical properties of silicone-alumina nanocomposites are shown and compared with those of unfilled matrix, used as a reference. The influence of different fillers content (1-7% in weight) on nanocomposites properties is fully discussed.*

### 1 Introduction

The increasing demand for higher operating temperatures, more severe duty cycles, smaller dimensions and the introduction of new technologies for the production of traction electrical motors have, in the last decade, enlarged the electrical, mechanical and thermal stresses over the dielectrics in power rotating machines thus determining an increased risk of faster degradation rates of the insulating materials, such as epoxy and silicone resin, widely used for the vacuum pressure impregnation (VPI) of motor windings [1, 2]. As a result, installed motors may experience an increase in the electrical insulation failure mostly due to dielectric breakdown between adjacent turns. In fact, the insulation of rotating machines is subjected to multiple and concomitant stresses, for example, electrical, mechanical, and thermal stresses [3]. The heat generated during operations might potentially affect the structural integrity of the final product, if it is not dissipated. Thus, the improvement of heat dissipation in electrical and electronic devices has recently become a very important issue. For such a reason efforts have been dedicated to the improvement of the insulation performances by enhancing the ability of the polymers to dissipate excess heat and by enhancing electrical endurance which would lead to less maintenance and longer components life.

Nanocomposites have found numerous applications in the areas of materials technology and mechanical engineering, but only recently [4] the development of new materials has been focused towards electrical insulation. It has been found that the enhancement of insulating

materials performances can be obtained by the inclusion in the polymer matrix of nano-sized solid particles, such as ceramics or metals. The modification of properties can be mainly attributed to the enormous specific interfacial area of nanoparticles inclusions since all mechanisms taking place at such interfaces can be significantly altered.

In recent years, while many results have been published in the literature about epoxy based nanocomposites [5-7], few data are still available about nano-filled silicone resin. The present paper is focused on the preparation and the morphological, thermal, mechanical and electrical characterization of new materials obtained by addition of nano-sized alumina ( $\text{Al}_2\text{O}_3$ ) fillers to silicone matrix. Their measured physical, mechanical and electrical properties are compared with those of the unfilled matrix.

## 2 Materials and testing methods

### 2.1 Silicone nanocomposites preparation

A commercial methyl-phenyl-vinyl hydrogen polysiloxane resin (supplied by Wacker Chemie) was selected as the host matrix. Alumina nanoparticles, with average particle size smaller than 50 nm ( $\text{Al}_2\text{O}_3$  supplied by Sigma Aldrich), were used for composites preparation (see table 1).

Nanocomposites containing 1, 3, 5 and 7 weight percent of alumina, with respect to the total mass of the silicone resin, were prepared in laboratory scale, according to combined dispersion techniques: mechanical mixing and sonication.

The as-received nanoparticles were first dispersed in the polymer matrix by mechanical mixing with a high speed homogenizer "Turrax T25" at 6500 rpm for 10 min. In a second step the application of ultrasonic wave with an ultrasonic processor, ("Hielscher UP200S") at a 50% of maximum amplitude (200W) for about 30 min, promotes the disruption of remaining aggregates due to the pressure oscillation with high frequency occurring in the composite. Finally, the sonicated mixture was degassed for removal of air bubbles.

Property	$\text{Al}_2\text{O}_3$	Silicone Resin
Density	3.98	1.13
Thermal conductivity [W/mK]	40	0.16
Electrical resistivity [ $\Omega$ cm]	$> 10^{14}$	$> 10^{16}$
Relative permittivity	6.0÷7.0	2.6
Surface area [ $\text{m}^2/\text{g}$ ]	35-43	
Average size [nm]	40-47	

**Table 1.** Properties of  $\text{Al}_2\text{O}_3$  and silicone resin.

Plane, disc-shaped samples, with a thickness ranging between 0.6 and 0.9 mm and diameter  $d=8$  cm, were prepared for preliminary electrical characterization.

Silicone nanocomposite containing 3%  $\text{Al}_2\text{O}_3$  in weight was used to impregnate specimens obtained from section of stator windings of medium voltage motors (see figure 1). This specimen reproduces a representative section of the stator of electrical motor and it is constituted by two copper insulated conductors. Each conductor is insulated by a layer (0.11 mm) of corona resistant kapton tape; the outer insulation is made out of layers of mica tape and the silicone resin nanocomposite is used for under vacuum impregnation of the whole sample (figure 1).

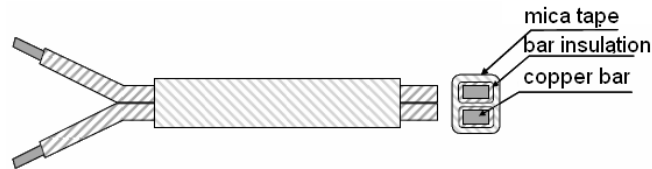


**Figure 1.** Sample for accelerated aging tests, supplied by Ansaldo Breda S.p.A

## 2.2 Characterization

Thermal stability of the samples was studied by thermogravimetric analysis (TGA) using a TA Instrument Q-5000 balance. The temperature was ramped at a rate of 10°C/min from room temperature up to 700°C in nitrogen atmosphere; initial thermal decomposition temperature ( $T_{id}$ ) was evaluated at 3% weight loss.

The thermal conductivity of neat silicone resin and nanocomposites has been estimated by modulated DSC (MDSC), using a TA Instruments DSC Q-1000 at 10°C/min heating rate,  $\pm 0,5^\circ\text{C}$  amplitude temperature modulation and a period of 80sec, according to ASTM E 1952 [8].

Dynamic-mechanical analysis was carried out by a TA Instruments DMA Q800 at a heating rate of 5°C/min, in a temperature range from  $-50^\circ$  to  $110^\circ\text{C}$ . Single cantilever geometry has been adopted, with a deformation amplitude of  $15\mu\text{m}$  at the frequency of 1 Hz.

Dc volume resistivity ( $\rho_v$ ) has been evaluated at  $23^\circ\text{C}$  by holding the specimens in a suitable shielded cell with guard ring electrodes and using a stabilized dc source and a picoammeter HP 4140B. Prior to the measurement, the specimen were held in an oven at the controlled temperature of  $30^\circ\text{C}$  for 48 hours. The voltage of 1400V, corresponding to an applied electrical field included in the interval from 15.5 to 23.0 kV/cm, was then applied across the samples. Readings of the conduction current were taken after 120 s from the application of the voltage, when a stable state was reached.

Relative dielectric permittivity ( $\epsilon_r$ ) and dissipation factor ( $\text{tg } \delta$ ) were measured at room temperature ( $23^\circ\text{C}$ ), high voltage (1.2 kV) and 50 Hz by placing the samples in a dielectric test cell Tettex 2914 and by adopting a Haefely bridge type 470.

The variations of relative permittivity ( $\epsilon_r$ ) and dissipation factor ( $\text{tg } \delta$ ) with respect to frequency were measured at room temperature ( $23^\circ\text{C}$ ) and low voltage (1.1 V) in the frequency range ( $102\div 106$  Hz) by using an impedance analyzer HP 4192A and a suitable test cell Agilent 16451B. The dielectric test fixture was equipped with a 4-terminal pair cable assembly and was used in the guarded electrode configuration. The reported data are an average value of 5 measurements.

Dielectric strength tests were carried with a Baur PGO-5E dielectric tester and by placing the specimen in oil between a couple of Rogowsky electrodes, in accordance with ASTM D149 [9].

The data presented in this paper are an average value of 5 samples.

## 3. Experimental results and discussion

### 3.1 Thermal Stability (TGA)

Initial thermal decomposition temperatures were reported in table 2 for all samples. It was observed that the addition of the inorganic fillers does not affect the degradation process, and a slight increase was presented for the nanocomposite with 1%  $\text{Al}_2\text{O}_3$  content.

### 3.2 Dynamic Mechanical Analysis (DMA)

Mechanical behavior of silicone resin and its nanocomposites was studied by DMA analysis. The storage modulus ( $E'$ ) and damping factor ( $\text{tan}\delta$ ) curves are shown in figures 3a and 3b,

respectively. The glass transition temperature ( $T_g$ ) (table 3) of the composites is identified at the maximum of  $\tan\delta$  curves.

Sample t	$T_{id}$ (3% weight loss) [°C]
Neat silicone	359
1% $Al_2O_3$	364
3% $Al_2O_3$	355
5% $Al_2O_3$	350
7% $Al_2O_3$	356

**Table 2.** Thermal stability of silicone nanocomposites at different  $Al_2O_3$  content.

The addition of ceramic particles determines a slight increase in the elastic modulus which, for the 7%wt samples, becomes  $\sim 10\%$  higher than the neat resin. On the contrary,  $T_g$  values decrease with filler content and reach a minimum for the 7%wt samples, characterized by a  $T_g$  value  $10^\circ C$  smaller than the unfilled resin.

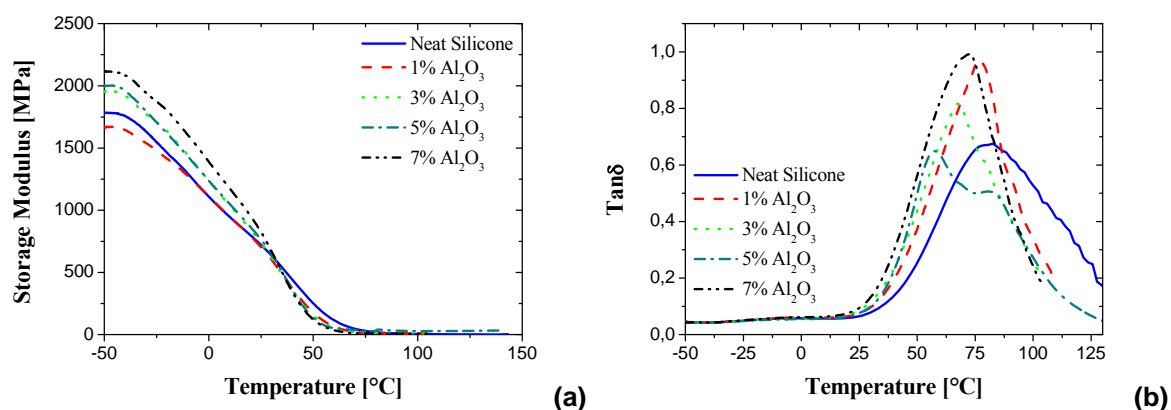


**Figure 3.** Storage modulus  $E'$  (a) and  $\tan\delta$  (b) curves of the silicone- $Al_2O_3$  nanocomposites.

Sample	$E'$ [GPa]	$T_g$ [°C]
Neat silicone	0.72	83
1% $Al_2O_3$	0.70	76
3% $Al_2O_3$	0.73	67
5% $Al_2O_3$	0.76	61
7% $Al_2O_3$	0.82	72

**Table 3.**  $E'$  and  $T_g$  values of silicone neat resin and its nanocomposites at different filler contents.

### 3.3 Thermal conductivity

Thermal conductivity values are evaluated from measurements of the heat capacity and apparent heat capacity of two samples of different geometry: cylinders with 6.3 mm in diameter and 0.4 mm and 3.5 mm of thickness, respectively. The thermal conductivity values for silicone composites are listed in table 4.

Sample	$\lambda$ [W/mK]
Neat silicone	0.16
1% $Al_2O_3$	0.19
3% $Al_2O_3$	0.23
5% $Al_2O_3$	0.24
7% $Al_2O_3$	0.26

**Table 4.** Thermal conductivity of silicone nanocomposites at different filler content.

The data are an average value of 3 measurements. Increasing Al<sub>2</sub>O<sub>3</sub> content up to 7%wt the  $\lambda$  value increases from 0.16 W/mK, for neat resin, to 0,26 W/mK for 7% Al<sub>2</sub>O<sub>3</sub> sample, corresponding to an increase of about 70% with respect to neat resin (see figure 4). This improvement, is probably due to the formation of a percolative pathway for heat conduction. In fact the mode of thermal conduction in amorphous polymer is mainly due to the presence of conductive paths formed by conductive particles and factors that influence the thermal conductivity can be the size, the amount and the shape of particles.

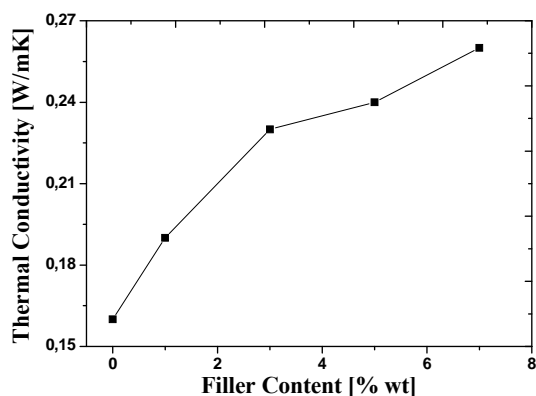


Figure 4. Thermal conductivity of the silicone-Al<sub>2</sub>O<sub>3</sub> nanocomposites.

### 3.4 dc volume resistivity $\rho_v$

Figure 5 shows the plot of dc volume resistivity  $\rho_v$  vs. the filler content. All values are shown in table 5.

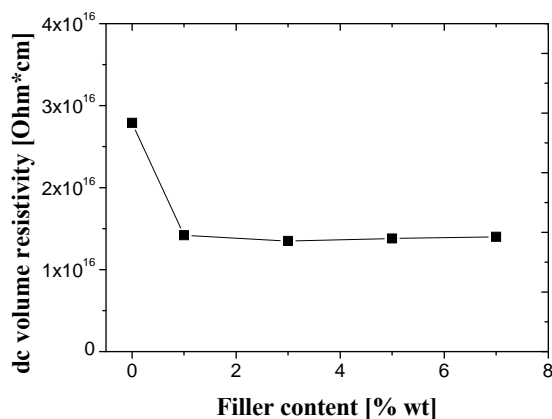


Figure 5. Variation of dc volume resistivity of the silicone-nanocomposites with respect to Al<sub>2</sub>O<sub>3</sub> content.

Sample	Volume Resistivity $\rho_v$
	[Ohm*cm]
Neat silicone	2.79*10 <sup>16</sup>
1% Al <sub>2</sub> O <sub>3</sub>	1.42*10 <sup>16</sup>
3%Al <sub>2</sub> O <sub>3</sub>	1.35*10 <sup>16</sup>
5%Al <sub>2</sub> O <sub>3</sub>	1.38*10 <sup>16</sup>
7%Al <sub>2</sub> O <sub>3</sub>	1.40*10 <sup>16</sup>

Table 5.  $\rho_v$  of silicone nanocomposites at different Al<sub>2</sub>O<sub>3</sub> content.

It can be seen that even the introduction of a small amount of filler reduces the dc resistivity value ( $\rho_v=2.8 \times 10^{16} \Omega\text{cm}$  for the neat resin and  $\rho_v=1.4 \times 10^{16} \Omega\text{cm}$  for the 1%wt composites), but the reduction can be estimated as not significant; for higher filler loading it remains practically unchanged.

### 3.5 Permittivity $\epsilon_r$ and dissipation factor $\text{tg } \delta$

The behavior of the insulating material when subjected to high electrical stresses at industrial frequency was evaluated by means of permittivity and dissipation factor trends. In particular the presence of losses due to partial discharge activity can be identified by comparing the values of  $\text{tg } \delta$  with those measured in low voltage tests. Results obtained as a function of the filler content, are reported in table 6.

Sample	$\epsilon_r$	$\text{tg } \delta$
Neat silicone	2.6	$1.7 \cdot 10^{-2}$
1% $\text{Al}_2\text{O}_3$	2.5	$1.5 \cdot 10^{-2}$
3% $\text{Al}_2\text{O}_3$	2.8	$1.5 \cdot 10^{-2}$
5% $\text{Al}_2\text{O}_3$	2.8	$1.4 \cdot 10^{-2}$
7% $\text{Al}_2\text{O}_3$	2.7	$2.4 \cdot 10^{-2}$

**Table 6.**  $\epsilon_r$  and  $\text{tg } \delta$  values of silicone nanocomposites at different  $\text{Al}_2\text{O}_3$  content.

At 1% wt filler content permittivity is lower than the unfilled resin. The reduction of permittivity value cannot be due to alumina nanoparticles since dielectric permittivity of alumina is around 7 and may ascribed to the restriction of polymer chain movement by nanoparticles. At higher filler content, permittivity increases. The difference is probably due to higher probability of finding clusters or agglomerates in the polymer matrix and interfacial effects are less pronounced. Dielectric losses are at the same level as in neat resin up to 5% wt. Since their contribution is given by conduction and polarization losses. It means that the presence of nano-fillers seems to inhibit losses.

### 3.6 Dielectric Spectroscopy

The variations of relative permittivity ( $\epsilon_r$ ) and dissipation factor ( $\text{tg } \delta$ ) with respect to frequency are shown in figures 6a e 6b for different filler concentrations. The results show an increase of permittivity with filler content and the absence of relevant relaxation phenomena for the nano-composites in the measured frequency range (fig. 6.a). Furthermore, the dissipation factor  $\text{tg } \delta$  is lower in the nano-composites than in the neat resin (fig. 6.b), showing as the presence of nano-fillers seems to inhibit losses at frequencies above 1 kHz.

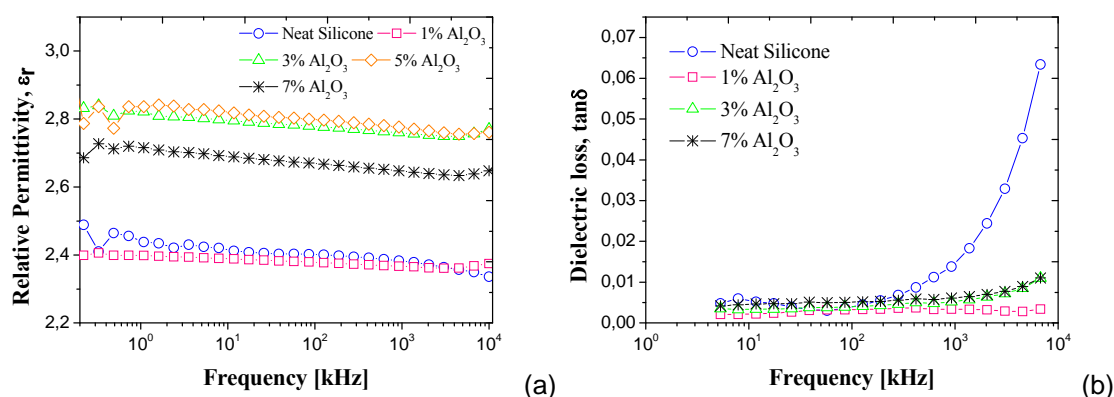


**Figure 6.** Frequency dependence of relative permittivity  $\epsilon_r$  (a) and dissipation factor  $\text{tg } \delta$  (b) of  $\text{Al}_2\text{O}_3$  nanocomposites.

### 3.7 Dielectric Strength

Figure 7 shows the dielectric strength vs. filler content for silicone nanocomposites. It can be observed that the dielectric strength decreases with increasing of  $\text{Al}_2\text{O}_3$  content. Moreover, the dispersion in the breakdown values is higher in the nanocomposites. Such a behavior can be ascribed to the presence of defects in the polymer matrix as consequence of the addition of nanoparticles.

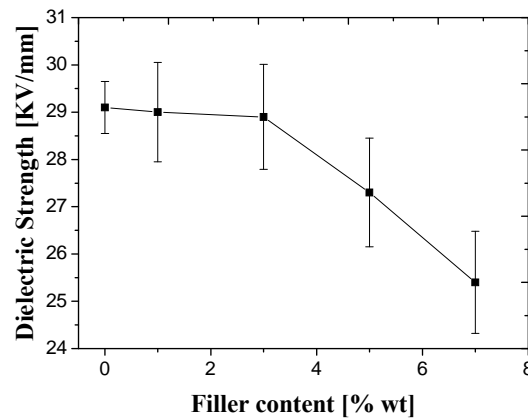


Figure 7. Variation of dielectric strength of silicone nanocomposites with respect to  $\text{Al}_2\text{O}_3$  content.

## 4. Conclusions

Results on the investigation of silicone nanocomposites based on ceramic alumina nanoparticles are presented. The presence of thermally conductive particles improves heat dissipation of thermosetting resins widely used for the vacuum pressure impregnation (VPI) of electrical motor.

The addition of alumina nanoparticles does not affect significantly the thermal stability of silicone nanocomposites. Although silicone resins exhibit elastic modulus lower than other thermosets, the addition of 7% in weight of alumina results in an 10% increase of elastic modulus with respect to neat resin.

An increase in thermal conductivity (about 40% with respect to neat resin) was obtained with the 3% wt composites, while leaving the mechanical and electrical characteristics almost unchanged. For this reason, according to requirements of Ansaldo Breda industry, 3% $\text{Al}_2\text{O}_3$  nanocomposite sample was chosen to impregnate a section of stator windings of electrical traction motors (see fig. 3).

At higher filler content (7% wt) the increase in thermal conductivity is even greater, but the drop in dielectric strength is a clear indication of the worsening of electrical properties. Such experimental findings and the higher values of relative permittivity can be probably due to the higher probability of finding clusters or aggregates of filler particles which act as defects or impurities inside the insulating matrix.

Moreover it appears an upper level for the electrical conductivity, in spite the thermal behaviour which doesn't show any saturation effect by increasing the filler content.

Dissipation factor spectra shows at high frequencies a significant reduction of the losses with respect to the neat resin. This behaviour can be probably ascribed to a sort of ion trapping, whose explanation deserves a deeper theoretical modelling.

Electrical strength of the nanocomposites show a significant lowering of the breakdown level beyond a critical value of the filler content.

## 5. Acknowledgements

The activities were performed in the frame of the project “PIROS” (DM 20162) granted to IMAST S.c.a.r.l. and funded by the M.I.U.R.

## References

- [1] M. Kaufhold, G. Börner, M. Eberhardt, J. Speck, Failure Mechanism of the Interturn Insulation of Low Voltage Electric Machines Fed by Pulse-Controlled Inverters, *IEEE Electrical Insulation Magazine*, **12**, pp. 9-16 (1996).
- [2] M. Melfi, A.M.J. Sung, S. Bell, G.L. Skibinski, Effect of surge voltage risetime on the insulation of low-voltage machines fed by PWM converters, *IEEE Trans. on Industry Applications*, **34**, pp. 66–775 (1998).
- [3] A. Omrani, L.C. Simon, A.A. Rostami, The effects of alumina nanoparticle on the properties of an epoxy resin system, *Mater Chem Phys*, **114**, pp. 145-150 (2009).
- [4] T. Tanaka, G.C. Montanari, R. Mulhaupt, Polymer nanocomposites as Dielectric and Electrical Insulation-perspectives for Processing Technologies, *Material Characterization and Future Applications*, *IEEE Trans. Dielectrics and Electrical Insulation*, **11**, pp. 763-784 (2004).
- [5] S. Singh, M. Joy Thomas, Dielectric Properties of Epoxy Nanocomposites, *IEEE Trans. Dielectrics and Electrical Insulation*, **15**, pp. 12-23 (2008).
- [6] I. Ramirez , E.A. Cherney , S. Jayaram , M. Gauthier, L. Simon, Erosion resistance and mechanical properties of silicone nanocomposite insulation, *IEEE Trans. Dielectrics and Electrical Insulation*, **16**, pp. 52-59 (2009).
- [7] E. Amendola, A.M. Scamardella, C. Petrarca, D. Acierno, Epoxy-Nanocomposites with ceramic reinforcement for electrical insulation, *Journal of Applied Polymer and Science*, **122**, pp. 3686-3693 (2011).
- [8] ASTM E 1952, *Standard Test Method for Thermal Conductivity and Thermal Diffusivity by Modulated Temperature Differential Scanning Calorimetry* (2001).
- [9] ASTM D149, *Standard Test Method for Dielectric Breakdown Voltage and Dielectric Strength of Solid Electrical Insulating Materials at Commercial Power Frequencies* (2004).